

Effect of alpha-particle irradiation dose on SiN_x/AlGaN/GaN metal–insulator semiconductor high electron mobility transistors


Chaker Fares, Fan Ren, Stephen J. Pearton, Gwangseok Yang, Jihyun Kim, Chien-Fong Lo, and J. Wayne Johnson

Citation: *Journal of Vacuum Science & Technology B* **36**, 041203 (2018); doi: 10.1116/1.5042261

View online: <https://doi.org/10.1116/1.5042261>

View Table of Contents: <http://avs.scitation.org/toc/jvb/36/4>

Published by the [American Vacuum Society](#)



Instruments for Advanced Science

Contact Hiden Analytical for further details:
W www.HidenAnalytical.com
E info@hiden.co.uk

CLICK TO VIEW our product catalogue




Gas Analysis

- dynamic measurement of reaction gas streams
- catalysis and thermal analysis
- molecular beam studies
- dissolved species probes
- fermentation, environmental and ecological studies




Surface Science

- UHV TPD
- SIMS
- end point detection in ion beam etch
- elemental imaging - surface mapping



Plasma Diagnostics

- plasma source characterization
- etch and deposition process reaction kinetic studies
- analysis of neutral and radical species



Vacuum Analysis

- partial pressure measurement and control of process gases
- reactive sputter process control
- vacuum diagnostics
- vacuum coating process monitoring

Effect of alpha-particle irradiation dose on SiN_x/AlGaIn/GaN metal–insulator semiconductor high electron mobility transistors

Chaker Fares and Fan Ren^{a)}

Department of Chemical Engineering, University of Florida, Gainesville, Florida 32611

Stephen J. Pearton

Department of Material Science and Engineering, University of Florida, Gainesville, Florida 32611

Gwangseok Yang and Jihyun Kim

Department of Chemical and Biological Engineering, Korea University, Seoul 136-713, South Korea

Chien-Fong Lo and J. Wayne Johnson

IQE, Taunton, Massachusetts 02780

(Received 30 May 2018; accepted 26 June 2018; published 11 July 2018)

The effects of 18 MeV alpha particle irradiation dose on the electrical properties of SiN_x/AlGaIn/GaN metal insulator semiconductor high electron mobility transistors (MISHEMTs) using *in situ* grown silicon nitride as the gate dielectric were investigated. The MISHEMT devices were irradiated with alpha particles at doses of 1×10^{12} or 1×10^{13} cm⁻² at a fixed energy of 18 MeV. Device performance degradation was more prominent for the irradiated samples under high frequency operation. At a frequency of 100 kHz and gate voltage pulsed from -6 to 3 V, the saturation drain current reduction was 32% and 41% after alpha irradiation doses of 1×10^{12} and 1×10^{13} cm⁻², respectively. The drain current reduction at 100 kHz also depended on the duty cycle. At higher duty cycles, the drain current reduction was less severe. The calculated carrier removal rates were in the range of 2062–2175 cm⁻¹ for the alpha doses studied. The results demonstrate the capability of AlGaIn/GaN MISHEMTs in environments where resilience to radiation is required. *Published by the AVS.* <https://doi.org/10.1116/1.5042261>

I. INTRODUCTION

The utilization of radiation-resistant microelectronics is necessary in applications such as radar technology, satellite-based communication, remote sensing, and nuclear energy production. As an example, primary cosmic rays, originating outside of Earth's atmosphere, are composed primarily of protons (90%) and alpha particles (9%), so the effect of these particles on microelectronics is of particular interest. Of the numerous device architectures and materials previously studied, AlGaIn/GaN high electron mobility transistors (HEMTs) show a higher radiation resistance than silicon based metal oxide field effect transistors (MOSFETs) and AlGaAs/GaAs based HEMTs due to the higher energy bandgap of nitrides.^{1–9} Despite the many advantages of AlGaIn/GaN HEMTs, these devices can exhibit gate-lag trapping effects on the AlGaIn surface and also frequently suffer from high gate leakage.^{10–15} To reduce gate leakage and boost gate swing, insulating dielectric layers such as Al₂O₃, HfO₂, SiO₂, and SiN_x have been implemented between the heterostructure interface and gate contact. While many gate dielectrics have been investigated, SiN_x deposited by plasma enhanced chemical vapor deposition has been the most widely used to passivate surface trap states and reduce drain current collapse.^{16–20} These metal insulator semiconductor high electron mobility transistors (MISHEMTs) successfully reduce gate leakage and yield higher breakdown voltages.^{21–23} The study of alpha irradiation dose on device performance is crucial to develop radiation-tolerant systems and establish long-life device reliability.^{24–27}

A few studies have been performed to analyze how HEMTs respond to irradiation damage, but the effects of alpha irradiation dose on MISHEMTs have not been investigated.^{26,28–32} For AlGaIn/GaN HEMTs irradiated with alpha particles at 2 MeV, a 35% reduction in the transconductance was observed at a dose of 1×10^{13} cm⁻², whereas a 70% reduction in transconductance was observed at a dose of 1×10^{14} cm⁻².³³ Ohyama *et al.*³⁴ studied the degradation effects of alpha irradiation dose on HEMTs and reported that the devices irradiated with larger doses showed larger degrees of degradation. Due to the scarcity of information on alpha irradiation effects on SiN_x/AlGaIn/GaN MISHEMTs, it is worth investigating the radiation hardness of these devices to alpha particle induced damage.

In this study, we present the first report on the effects of alpha irradiation dose on gate and drain current–voltage characteristics, sheet resistance, contact resistance, mobility, carrier removal rate, and gate-pulsed characteristics of SiN_x/AlGaIn/GaN MISHEMTs.

II. EXPERIMENT

The AlGaIn/GaN MISHEMT structure consisted of a 9 nm *in situ* SiN_x insulating layer, an 18 nm AlGaIn barrier layer, a 200 nm GaN channel layer, a 4200 nm GaN buffer layer, and a 180 nm AlN nucleation layer fabricated by metal organic chemical vapor deposition on an 8 in Si substrate. For the MISHEMT fabrication, source and drain regions were formed by deposition of Ti/Al/Ni/Au Ohmic contacts annealed at 850 °C in flowing N₂. The device isolation was achieved by multiple energies and doses of nitrogen ion

^{a)}Electronic mail: fren@che.ufl.edu

implantation.³⁵ Electron beam deposited Ni/Au based metalization was utilized for $2\ \mu\text{m}$ gate-length Schottky gates. The device layers and architecture are shown in Fig. 1.

Alpha irradiation was performed at the Korean Institute of Radiological and Medical Sciences (KIRAMS) using a MC 50 (Scanditronix) cyclotron. The alpha particle energy at the outlet of the cyclotron was 30 MeV. The alpha particle energies were adjusted prior to hitting the sample by passing through several aluminum degraders. The beam currents were measured using a Faraday-cup which was also used to calculate the flux density.

The device DC characteristics before and after irradiation were performed with a HP 4156 parameter analyzer, and the pulse measurement was conducted with an Agilent 8114A pulse generator, a Hewlett-Packard E3615A power supply, and an Agilent Infinium oscilloscope. Capacitance–voltage measurements were performed with an Agilent 4284A Precision LCR Meter.

III. RESULTS AND DISCUSSION

A stopping and range of ions in matter simulation (SRIM) was used to simulate the vacancy density and distribution generated from alpha particles at each corresponding dose investigated. The total thickness of the samples investigated was $1000\ \mu\text{m}$, and at 18 MeV, the alpha particles had a maximum penetration depth of $190\ \mu\text{m}$. The stopping mechanism of the alpha particles with the irradiation energy used in this study was dominated by nuclear stopping. Nuclear stopping is elastic and dominates at lower irradiation energies, unlike electronic stopping which primarily results in heat generation and minimal defect formation.^{8,36–38} The energy lost during nuclear stopping is transferred to the target atom which is then recoiled away from its lattice site, causing crystal lattice disorder within the sample.^{8,36,39} Figure 2 illustrates the simulated number of vacancies within the two dimensional electron gas (2DEG) channel region of the MISHEMT devices as a function of alpha irradiation dose. The effect of alpha particle dose on device performance in MISHEMT devices is primarily determined by the defect concentration within the active layers of the device. The 2DEG channel within the MISHEMT devices investigated is located $27\ \text{nm}$ from the surface, and vacancies created around this region are the primary cause of current degradation due to carrier trapping and the effect on mobility.

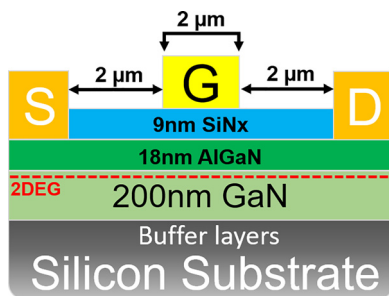


Fig. 1. (Color online) Schematic of the AlGaIn/GaN MISHEMT device used in this study.

Table I shows the contact resistivity and sheet resistance of the AlGaIn/GaN MISHEMTs derived from transmission line measurement (TLM) data as a function of alpha irradiation dose. The data points shown in Table I represent an average of eight separate TLM measurements. After an alpha particle dose of $1 \times 10^{12}\ \text{cm}^{-2}$, the contact resistance and sheet resistance increased 9.1% and 3.5%, respectively. The increase in these resistances is consistent with the simulated concentration of vacancies within the 2DEG channel. The vacancies generated by irradiation result in an increased resistance due to a reduction of the carrier mobility and a decreased free electron concentration. With regard to the contact resistance, more severe degradation compared to the sheet resistance was observed at both alpha particle doses. For MISHEMTs irradiated with an alpha particle dose of $1 \times 10^{13}\ \text{cm}^{-2}$, the contact resistance increased 11.42%. The larger degree of degradation in the contact resistance could be due to the damage in the epilayers beneath the Ohmic contacts prior to irradiation in the fabrication of the MISHEMT devices. During the high temperature annealing step for Ohmic contact formation, the heterojunction interface reacts with the Ohmic metal, causing metal diffusion and agglomeration. These annealing induced defects are then susceptible to further damage from irradiation particles scattering through the metal interface.

Figure 3 illustrates the drain I-V behavior of the AlGaIn/GaN MISHEMT devices before and after alpha irradiation at 18 MeV with a dose of $1 \times 10^{13}\ \text{cm}^{-2}$. The gate was biased starting from 3 V and was stepped down in 1-V increments, whereas the drain voltage was swept from 0 to 10 V at each corresponding gate voltage. The main cause of DC degradation in the irradiated devices resulted from charged trap generation within GaN channel and AlGaIn barrier layers. As charged traps are created within the GaN and AlGaIn layers, the potential difference between the Fermi level (E_F) and the ground state of sub-bands (E_0) decreases, causing conduction band bending, which resulted in a lower sheet carrier concentration.^{40,41} Additionally, a reduced electron density within the 2DEG channel and a lower carrier mobility could have contributed to the reduced DC performance.^{26,29,42} The amount of dc degradation is consistent with the TLM results,

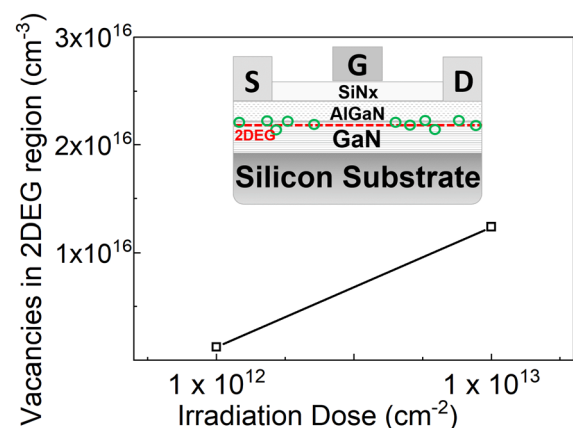


Fig. 2. (Color online) SRIM simulations showing vacancies created within the 2DEG region as a function of alpha irradiation dose.

TABLE I. Sheet and contact resistances before and after alpha irradiation at doses of 1×10^{12} or $1 \times 10^{13} \text{ cm}^{-2}$ at a fixed energy of 18 MeV.

Irradiation dose (cm^{-2})	R_S (Ω/\square)	R_c ($\Omega \text{ cm}^2$)
Reference	416.80	8.58×10^{-6}
1×10^{12}	431.58	9.36×10^{-6}
1×10^{13}	442.01	9.56×10^{-6}

with samples irradiated with a dose of $1 \times 10^{13} \text{ cm}^{-2}$ having an average reduction in saturation current of 10.7%.

Table II shows the electron mobility extracted from the low field drain I-V curves before and after alpha particle irradiation. The low-field linear region of the drain I-V measurements was utilized to extract the electron mobility, which was calculated using the following equation:

$$\frac{V_{DS}}{I_{DS}} = R_S + R_D + \frac{Ld}{\mu W \epsilon \epsilon_0 (V_{GS} - V_{OFF})}, \quad (1)$$

where V_{DS} is the drain voltage, I_{DS} is the drain current, R_S and R_D are the source and drain resistances, respectively, L is the gate length, d is the equivalent gate dielectric thickness depth of SiN_x and AlGaIn layers, W is the gate width, ϵ_0 is the absolute permittivity, ϵ is the equivalent dielectric constant of the SiN_x and AlGaIn layers, V_{GS} is the gate voltage, μ is the electron mobility, and V_{OFF} is the threshold voltage. There was approximately a 13.6% and 24.3% decrease in carrier mobility for MISHEMTs irradiated with alpha particles at doses of 1×10^{12} and $1 \times 10^{13} \text{ cm}^{-2}$, respectively.

Figure 4 shows the drain current and normalized extrinsic transconductance as a function of the gate voltage for the $\text{AlGaIn}/\text{GaIn}$ MISHEMTs before and after alpha particle irradiation. The maximum extrinsic transconductances were reduced by 6.7% and 9.8% for MISHEMTs irradiated with alpha particle doses of 1×10^{12} and $1 \times 10^{13} \text{ cm}^{-2}$, respectively. The degradation of the transconductance had a similar but less severe effect than the saturation drain current reduction.

Figure 5 illustrates the drain and gate current of the MISHEMT devices before and after alpha irradiation at a

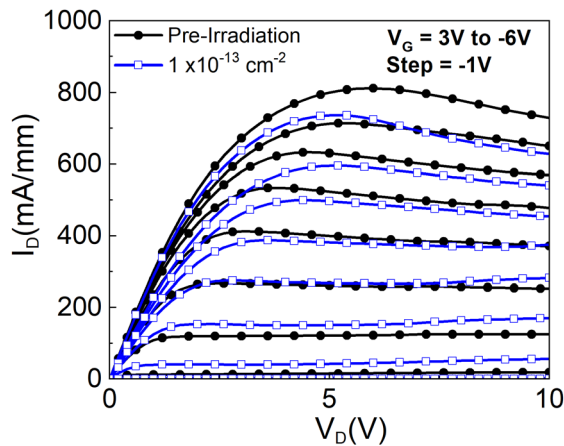


FIG. 3. (Color online) Drain I-V characteristics of MISHEMT samples irradiated with alpha particles at 18 MeV and a dose of $1 \times 10^{13} \text{ cm}^{-2}$ compared to the samples before irradiation.

TABLE II. Effect of alpha irradiation dose on the mobility of $\text{SiN}_x/\text{AlGaIn}/\text{GaIn}$ MISHEMTs.

Irradiation dose (cm^{-2})	Mobility ($\text{cm}^2/\text{V s}$)
Reference	1320
1×10^{12}	1140
1×10^{13}	998

fixed drain voltage of 10 V. The drain current on-off ratio indicates the quality of charge modulation in the two-dimensional electron gas channel as well as the power added efficiency, linearity, noise figure, and device reliability.⁴³ The I_{ON}/I_{OFF} ratio of the MISHEMTs was 4.06×10^7 prior to alpha irradiation but degraded to 5.2% and 10.1% after irradiation with alpha particle doses of 1×10^{12} and $1 \times 10^{13} \text{ cm}^{-2}$, respectively. Subthreshold swing measurements were used to identify the trap densities in the gate modulated region of the MISHEMTs.⁴⁴ The MISHEMT samples before irradiation exhibited a subthreshold slope of 86 mV/decade, whereas the samples after alpha irradiation had a slope of 110 and 115 mV/decade after doses of 1×10^{12} and $1 \times 10^{13} \text{ cm}^{-2}$, respectively. This increase is expected and agrees with the decrease in mobility and saturation current.

Capacitance–voltage measurements were utilized to measure the carrier concentration using the following equation:⁴⁵

$$N_D = \frac{2}{q \epsilon_s \epsilon_0 A^2} \frac{d\left(\frac{1}{C^2}\right)}{dV}, \quad (2)$$

where A is the Schottky area, ϵ_s is the equivalent dielectric constant of SiN_x and AlGaIn , ϵ_0 is the absolute permittivity, q is the elementary charge, C is the capacitance, and V is the voltage. Table III shows the carrier concentration reduction, sheet carrier concentration, and carrier removal rate of the alpha particle irradiated MISHEMTs. The trend of the carrier concentration reductions is consistent with the reduction of the electron mobility and saturation drain current. The

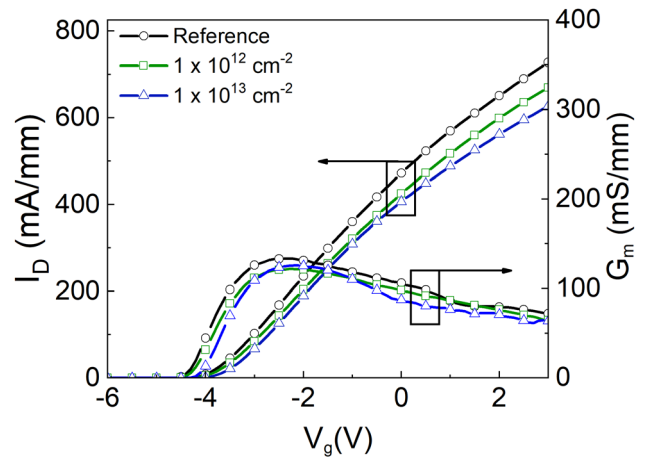


FIG. 4. (Color online) DC transfer characteristics before and after alpha particle irradiation.

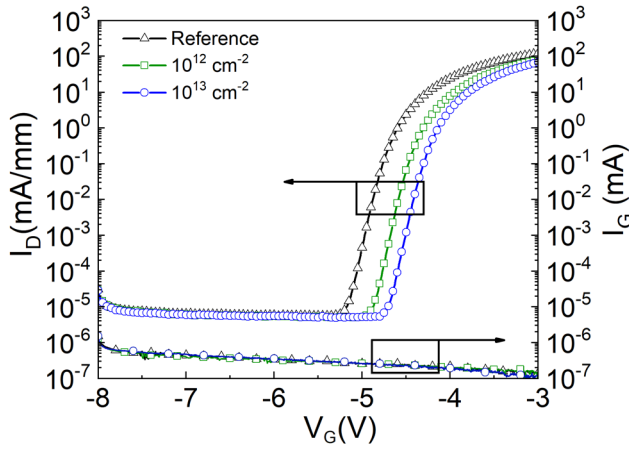


FIG. 5. (Color online) Subthreshold characteristics for MISHEMT devices pre- and postirradiation.

carrier removal rate was determined using the difference in the carrier concentration before and after the alpha irradiation normalized by the alpha irradiation dose. The calculated carrier removal rates were in the range of 2062–2175 cm⁻¹ for alpha doses studied. By comparison, protons of similar energy produce carrier removal rates approximately half these values in AlGaIn/GaN HEMTs.

Figure 6(a) shows gate-lag measurements used to quantify the effect of surface traps of the AlGaIn/GaN MISHEMTs before and after alpha particle irradiation. For the gate-lag measurement, a constant voltage of 5 V was applied to the device drain, while the gate was pulsed from -6 V to the gate voltage of interest. The voltage sweep was repeated for duty cycles of 10%–50% using increments of 10, while the frequency was kept constant at 100 kHz. Figure 6(b) shows the dc current and gate-pulsed characteristics of the MISHEMT samples irradiated with an alpha dose of 1 × 10¹² cm⁻². At a frequency of 100 kHz and 50% duty cycle, the saturation drain current reduction was 32% and 41% after alpha irradiation doses of 1 × 10¹² cm⁻² and 1 × 10¹³ cm⁻², respectively. In the off state, hot electrons are accelerated by the large voltage potential and become trapped at the interface between the SiN_x passivation layer and the HEMT surface. These trapped charges form a virtual gate between the gate and drain electrode. The virtual gate, also known as a surface depletion region, caused a reduced drain-current in the MISHEMTs which was most severe in the samples irradiated with a dose of 1 × 10¹³ cm⁻² due to a larger degree of surface damage. At lower duty cycles, the drain current reductions were more severe. As the duty cycle is decreased, the device is in the off-

TABLE III. Carrier concentration reduction, sheet carrier concentration, and carrier removal rate before and after alpha irradiation at a fixed energy of 18 MeV with a dose of 1 × 10¹² or 1 × 10¹³ cm⁻².

Irradiation dose (cm ⁻²)	Δ Carrier concentration reduction (%)	Sheet carrier concentration (cm ⁻²)	Carrier removal rate (cm ⁻¹)
Preirradiation	—	1.26 × 10 ¹³	—
1 × 10 ¹²	3.0	1.19 × 10 ¹³	2062
1 × 10 ¹³	8.2	1.11 × 10 ¹³	2175

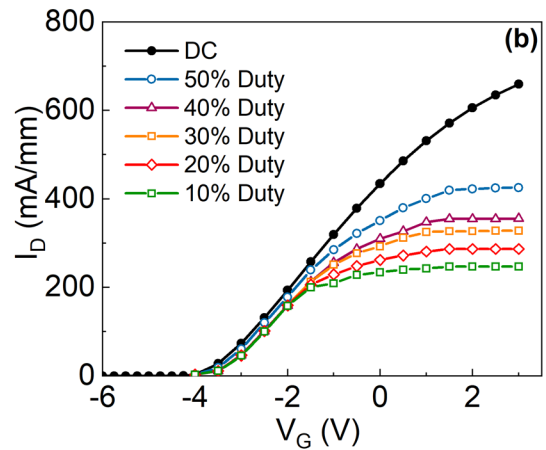
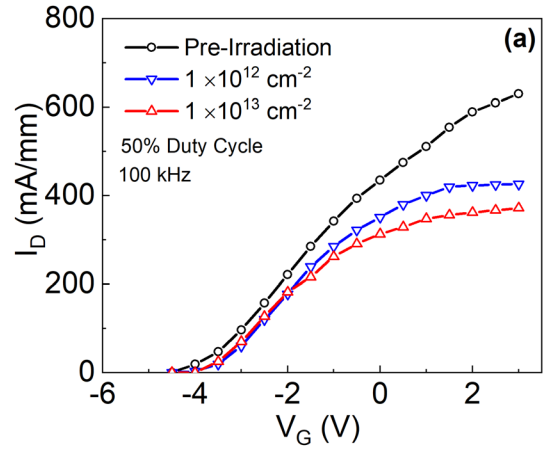


FIG. 6. (Color online) (a) Pulsed characteristics of MISHEMTs before and after alpha irradiation. (b) Gate-lag measurements of MISHEMT sample after alpha irradiation at a dose of 1 × 10¹² cm⁻² as a function of the duty cycle.

state for a longer period of time. For example, at a duty cycle of 10%, the device is on for 10% of the period and off for 90% of the period. As the device is held in the off-state for longer periods of time, a larger quantity of hot electrons travel to the surface and become trapped by dangling bonds. At a duty cycle of 10%, the current reduction in the MISHEMTs was 62% and 78% for devices irradiated with doses of 1 × 10¹² and 1 × 10¹³ cm⁻², respectively.

IV. SUMMARY AND CONCLUSIONS

The effect of alpha irradiation dose on AlGaIn/GaN MISHEMTs with *in situ* SiN_x cap layers was studied at a fixed irradiation energy of 18 MeV with doses of 1 × 10¹² or 1 × 10¹³ cm⁻². As the irradiation dose increases, the drain saturation current, maximum transconductance, mobility, sheet-carrier concentration, and high-frequency current retention decrease. Sheet resistance, transfer resistance, contact resistance, and threshold voltage all increased proportionally to the alpha irradiation dose. All AlGaIn/GaN MISHEMTs passivated with SiN_x were functional after alpha irradiation and could be pinched off. The GaN based MISHEMTs reported in this study have a radiation hardness over an order of magnitude larger than their GaAs based counterparts. For applications such as satellite communication and military radar

where radiation hard devices are required, AlGaIn/GaN MISHEMTs show impressive resistance to high energy alpha-induced device degradation.

ACKNOWLEDGMENTS

This project was sponsored by the Department of the Defense, Defense Threat Reduction Agency, HDTRA1-17-1-011, monitored by Jacob Calkins. The content of the information does not necessarily reflect the position or the policy of the federal government, and no official endorsement should be inferred. The research at Korea University was supported by the New and Renewable Energy Core Technology Program of the Korea Institute of Energy Technology Evaluation and Planning (KETEP) grant from the Ministry of Trade, Industry, and Energy, Republic of Korea (Nos. 20173010012970 and 20172010104830).

- ¹X. L. Wang, C. M. Wang, G. X. Hu, J. X. Wang, T. S. Chen, G. Jiao, J. P. Li, Y. P. Zeng, and J. M. Li, *Solid-State Electron.* **49**, 1387 (2005).
- ²Y. Irokawa *et al.*, *Appl. Phys. Lett.* **84**, 2919 (2004).
- ³S. J. Pearton, F. Ren, A. P. Zhang, and K. P. Lee, *Mater. Sci. Eng. R Rep.* **30**, 55 (2000).
- ⁴S. C. Binari, K. Ikossi, J. A. Roussos, W. Kruppa, D. Park, H. B. Dietrich, D. D. Koleske, A. E. Wickenden, and R. L. Henry, *IEEE Trans. Electron Devices* **48**, 465 (2001).
- ⁵R. J. Trew, *IEEE Microwave* **1**, 46 (2000).
- ⁶S. R. Messenger, E. A. Burke, G. P. Summers, M. A. Xapsos, R. J. Walters, E. M. Jackson, and B. D. Weaver, *IEEE Trans. Nucl. Sci.* **46**, 1595 (1999).
- ⁷G. H. Kinchin and R. S. Pease, *Rep. Prog. Phys.* **18**, 301 (1955).
- ⁸J. F. Ziegler and J. P. Biersack, *Treatise Heavy-Ion Science* (Springer, Boston, MA, 1985), pp. 93–129.
- ⁹D. Bräunig and F. Wulf, *Radiat. Phys. Chem.* **43**, 105 (1994).
- ¹⁰A. Mimouni, T. Fernández, J. Rodríguez-Tellez, A. Tazon, H. Baudrand, and M. Boussuis, *Electr. Electron. Eng.* **2**, 397 (2013).
- ¹¹Y.-S. Lin, Y.-W. Lain, and S. S. H. Hsu, *IEEE Electron Device Lett.* **31**, 102 (2010).
- ¹²G. Meneghesso, F. Rampazzo, P. Kordos, G. Verzellesi, and E. Zanoni, *IEEE Trans. Electron Devices* **53**, 2932 (2006).
- ¹³G. Meneghesso, G. Verzellesi, F. Danesin, F. Rampazzo, F. Zanon, A. Tazzoli, M. Meneghini, and E. Zanoni, *IEEE Trans. Device Mater. Reliab.* **8**, 332 (2008).
- ¹⁴J. W. Chung, J. C. Roberts, E. L. Piner, and T. Palacios, *IEEE Electron Device Lett.* **29**, 1196 (2008).
- ¹⁵J. Joh and J. A. del Alamo, *2006 International Electron Devices Meeting*, San Francisco, CA, 2006, pp. 1–4.
- ¹⁶K.-Y. R. Wong *et al.*, *2015 IEEE International Electron Devices Meeting* (IEEE, Washington, DC, 2015), pp. 9.5.1–9.5.4.
- ¹⁷Z. H. Liu, G. I. Ng, S. Arulkumaran, Y. K. T. Maung, K. L. Teo, S. C. Foo, and S. Vicknesh, *IEEE Electron Device Lett.* **32**, 318 (2011).
- ¹⁸B. M. Green, K. K. Chu, E. M. Chumbes, J. A. Smart, J. R. Shealy, and L. F. Eastman, *IEEE Electron Device Lett.* **21**, 268 (2000).
- ¹⁹J. Ma, X. Lu, X. Zhu, T. Huang, H. Jiang, P. Xu, and K. M. Lau, *J. Cryst. Growth* **414**, 237 (2015).
- ²⁰K. Cheng, S. Degroote, M. Leys, F. Medjdoub, J. Derluyn, B. Sijmus, M. Germain, and G. Borghs, *J. Cryst. Growth* **315**, 204 (2011).
- ²¹J.-C. Gerbedoen, A. Soltani, M. Mattalah, M. Moreau, P. Thevenin, and J.-C. De Jaeger, *Diamond Relat. Mater.* **18**, 1039 (2009).
- ²²S. Yagi, M. Shimizu, M. Inada, Y. Yamamoto, G. Piao, H. Okumura, Y. Yano, N. Akutsu, and H. Ohashi, *Solid-State Electron.* **50**, 1057 (2006).
- ²³A. Endoh, Y. Yamashita, N. Hirose, K. Hikosaka, T. Matsui, S. Hiyamizu, and T. Mimura, *Jpn. J. Appl. Phys., Part 1* **45**, 3364 (2006).
- ²⁴X. Hu *et al.*, *IEEE Trans. Nucl. Sci.* **51**, 293 (2004).
- ²⁵L. Liu *et al.*, *J. Vac. Sci. Technol.* **31**, 022201 (2013).
- ²⁶X. Hu *et al.*, *IEEE Trans. Nucl. Sci.* **50**, 1791 (2003).
- ²⁷B. Luo *et al.*, *J. Electron. Mater.* **31**, 437 (2002).
- ²⁸G. Sonia *et al.*, *Solid-State Electron.* **52**, 1011 (2008).
- ²⁹H.-Y. Kim, J. Kim, S. P. Yun, K. R. Kim, T. J. Anderson, F. Ren, and S. J. Pearton, *J. Electrochem. Soc.* **155**, H513 (2008).
- ³⁰S. Ahn *et al.*, *J. Vac. Sci. Technol.* **33**, 051208 (2015).
- ³¹S. Ahn, B.-J. Kim, Y.-H. Lin, F. Ren, S. J. Pearton, G. Yang, J. Kim, and I. I. Kravchenko, *J. Vac. Sci. Technol.* **34**, 051202 (2016).
- ³²H.-Y. Kim, J. Kim, L. Liu, C.-F. Lo, F. Ren, and S. J. Pearton, *J. Vac. Sci. Technol.* **30**, 012202 (2012).
- ³³F. Danesin, F. Zanon, S. Gerardin, F. Rampazzo, G. Meneghesso, E. Zanoni, and A. Pacagnella, *Microelectron. Reliab.* **46**, 1750 (2006).
- ³⁴H. Ohyama *et al.*, *IEEE Trans. Nucl. Sci.* **47**, 2546 (2000).
- ³⁵C. F. Lo, T. S. Kang, L. Liu, C. Y. Chang, S. J. Pearton, I. I. Kravchenko, O. Laboutin, J. W. Johnson, and F. Ren, *Appl. Phys. Lett.* **97**, 262116 (2010).
- ³⁶T. P. Ma and P. V. Dressendorfer, *Ionizing Radiation Effects in MOS Devices and Circuits* (Wiley, 1989).
- ³⁷S. T. Pantelides *et al.*, *Solid-State Electron.* **54**, 841 (2010).
- ³⁸B. R. Tuttle, D. R. Hughart, R. D. Schrimpf, D. M. Fleetwood, and S. T. Pantelides, *IEEE Trans. Nucl. Sci.* **57**, 3046 (2010).
- ³⁹J. R. Srour and J. M. McGarrity, *Proc. IEEE* **76**, 1443 (1988).
- ⁴⁰T.-S. Kang, F. Ren, B. P. Gila, S. J. Pearton, E. Patrick, D. J. Cheney, M. Law, and M.-L. Zhang, *J. Vac. Sci. Technol.* **33**, 061202 (2015).
- ⁴¹C. Claeys and E. Simoen, *Radiation Effects in Advanced Semiconductor Materials and Devices* (Springer, Berlin/Heidelberg, 2002).
- ⁴²A. P. Karmarkar, B. Jun, D. M. Fleetwood, R. D. Schrimpf, R. A. Weller, B. D. White, L. J. Brillson, and U. K. Mishra, *IEEE Trans. Nucl. Sci.* **51**, 3801 (2004).
- ⁴³S. J. Pearton, J. C. Zolper, R. J. Shul, and F. Ren, *J. Appl. Phys.* **86**, 1 (1999).
- ⁴⁴L. Liu *et al.*, *J. Vac. Sci. Technol.* **29**, 060603 (2011).
- ⁴⁵H. Arora, D. S. Rawal, and B. K. Sehgal, *Physics of Semiconductor Devices* (Springer, Cham, 2014), pp. 91–93.